ROLE OF MODULATION OF THE MITOCHONDRIAL QUALITY CONTROL IN HYPERTENSION-INDUCED HEART FAILURE

Ph.D. Thesis

Author: Orsolya Horváth

Program leader: Prof. Kálmán Tóth, M.D., D.Sc.
Project Leaders: Prof. Róbert Halmosi M.D., D.Sc.
László Deres Ph.D.

1st Department of Medicine
University of Pécs, Medical School
Hungary

2021

ABBREVIATIONS

ADP	adenosine diphosphate
Akt	protein kinase B
AMPK	AMP-activated protein kinase
ANOVA	analysis of variance
ATP	adenosine triphosphate
BGP-15	O-[3-piperidino-2-hydroxy-1-propyl]-nicotinic acid amidoxime dihydrochloride
BNP	brain-derived natriuretic peptide
COX1	cytochrome c oxidase subunit 1
COX3	cytochrome c oxidase subunit 3
CREB	cAMP response element-binding protein
DRP1	dynamin-related protein 1
DUSPs	dual-specificity phosphatases
E	mitral peak velocity of early diastolic filling
E'	early diastolic mitral annular velocity
ECM	extracellular matrix
EF	ejection fraction
ERK1/2	extracellular signal-regulated kinase 1/2
ETC	electron transport chain, mitochondrial
Fis1	mitochondrial fission 1 protein
GSK-3β	glycogen synthase kinase 3 beta
H_2O_2	hydrogen peroxide
HF	heart failure
IFM	interfibrillar mitochondria
IMM	inner mitochondrial membrane
JNK	c-jun N-terminal kinase
LV	left ventricle
LVEDV	left ventricular end-diastolic volume
LVEF	left ventricular ejection fraction
LVESV	left ventricular end-systolic volume
LVIDd	left ventricular end-diastolic inner diameter
LVIDs	left ventricular end-systolic inner diameter
MAPKs	mitogen-activated protein kinases

Mfn1/2	mitofusins 1 and 2
MKP-1	MAPK phosphatase-1
NADH	nicotinamide adenine dinucleotide
NRCM	neonatal rat cardiomyocytes
OMM	outer mitochondrial membrane
OPA1	optic atrophy 1
PARP-1	poly(ADP-ribose) polymerase-1
PGC-1α	peroxisome proliferator-activated receptor - γ coactivator-1α
PI3K	phosphatidylinositol 3-kinase
PKA	protein kinase A
PKC	protein kinase C
PW	posterior wall of the left ventricle
ROS	reactive oxygen species
SHR	Spontaneously hypertensive rat
TGF-β	transforming growth factor-beta
TNF-α	tumor necrosis factor-alpha
VDAC	voltage-dependent anion channel
WKY	Wistar-Kyoto rats

1. INTRODUCTION

Heart failure (HF) is a complex clinical syndrome where the functionally or structurally damaged heart is unable to maintain the proper cardiac output despite the growing number of therapeutic approaches, moreover the number of hospitalizations for HF as well as the HF associated mortality is increasing, thereby placing a heavy burden on health services and economy.

Hypertension is the most important risk factor resulting in abnormal loading conditions. Sustained elevation of blood pressure induces myocardial remodelling, which is characterized by interstitial fibrosis and cardiomyocyte hypertrophy. These cellular alterations are promoted by oxidative stress and by the activation of various intracellular signal transduction pathways. Numerous studies have demonstrated that mitochondria, which are responsible for the cellular energy supply, are also damaged in hypertension-induced cardiac remodelling and heart failure. Reactive oxygen species (ROS) induced mitochondrial DNA damage can be found in the background of these injuries and mitochondria themselves become the main sources of endogenous ROS production. The long-term presence of these pathophysiological factors can finally lead to heart failure (Fig.1).

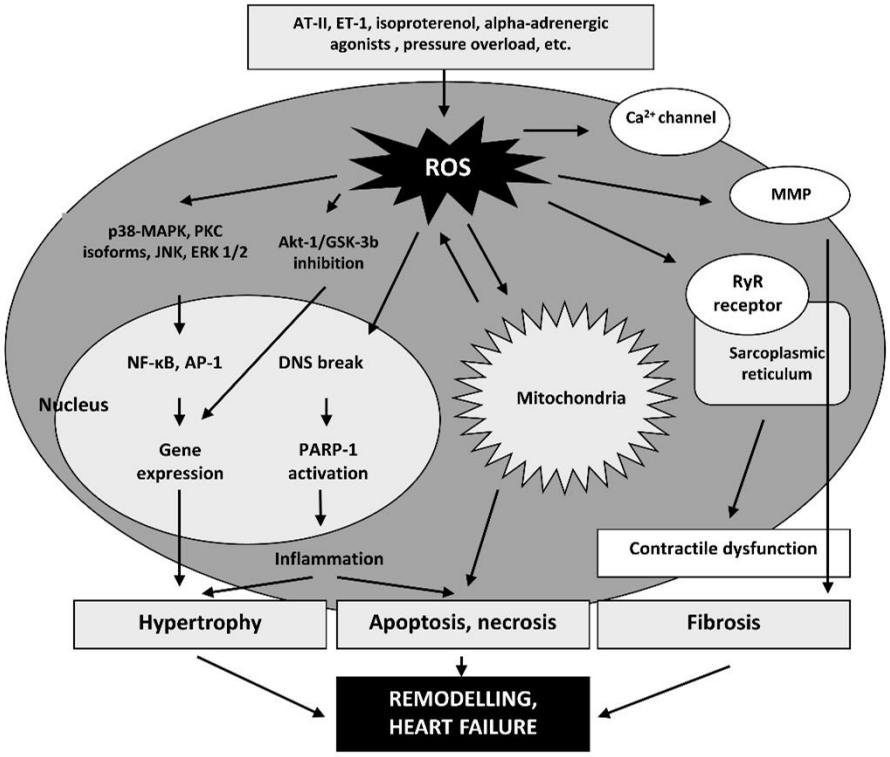

Figure 1. The role of oxidative stress in myocardial remodelling at heart failure

Treating heart failure, despite the numerous therapeutic possibilities, appears to be a challenging task nowadays. The major goal during the treatment is to improve the quality of life and functional capacity as well as to prevent hospital admissions and to try to reduce mortality. Beta blockers, angiotensin-converting enzyme inhibitors and mineralocorticoid receptor antagonist represent the main groups of

therapeutic possibilities. In spite of these approaches, the prognosis of the HF is still poor, and we do not have a proven beneficial option for the treatment of diastolic HF yet. Therefore, finding novel therapeutic targets and developing new compounds are extremely important to improve the outcome of HF in the future.

1.1 The role of signal transduction factors in the process of oxidative cell damage and in cardiovascular remodelling

During oxidative stress, the production of the free radicals is increased while the endogenous antioxidant system is not able to protect against them adequately. ROS seem to play a decisive role in the progression of pathological cardiac hypertrophy to heart failure via activating different transcriptions factors and signalling pathways. Heart failure can be seen as a final common state of various cardiac diseases, for example, hypertension, cardiomyopathies and valvular heart diseases.

Cardiac remodelling is referred to as a group of molecular, cellular and interstitial changes that manifest clinically as changes in size, mass (hypertrophy and atrophy), geometry (heart wall thickness), fibrosis and function of the heart after injury. Cardiac remodelling can be divided into two major groups, the physiologic and the pathologic remodelling. Physiologic remodelling can be characterized by adaptive hypertrophy and is not accompanied by cardiac fibrosis. During adaptive hypertrophy, the activation of phosphatidylinositol 3-kinase (PI3K) and protein kinase B (Akt) can be seen. Akt-1 belongs to prosurvival signalling factors and can promote the physiological hypertrophy, however it inhibits the pathological hypertrophy that is mainly characterized by cardiac collagen accumulation. Glycogen synthase kinase 3 beta (GSK-3β) is a downstream target of Akt-1 and Akt-1 can trigger the survival of chronically stressed cardiomyocytes in heart failure via the phosphorylation of GSK-3β. Due to increased phosphorylation of Akt-1 and GSK-3β, the cytoprotective impact is mediated via their protective effect on the structure and function of mitochondria. Moreover, the extracellular signal-regulated kinase 1/2 (ERK1/2) is also activated, which is responsible for hypertrophic growth. Based on the fact that ERK1/2 is a member of prosurvival signalling factors, its activation is beneficial in the failed myocardium.

Hypertension results in abnormal loading conditions and therefore can lead to the development of left ventricular hypertrophy and finally to heart failure, and it is associated with increased production of tumor necrosis factor-α (TNF-α) and angiotensin II. Protein kinase C (PKC) and the members of mitogen-activated protein kinase cascades (MAPKs) family, such as ERK1/2, C-jun N-terminal kinase (JNK) and p38 MAPK are all involved in cardiac remodelling. It is well known that MAPK signalling pathway plays an important role in the pathogenesis of hypertension-induced cardiac remodelling and heart failure. MAP kinases, predominantly p38 MAPK and JNK are also regulators of myocardial fibrosis. The activity of MAP kinases is regulated by dual-specificity phosphatases (DUSPs) or MAPK phosphatases (MKPs) that can dephosphorylate MAPKs and in this way can inhibit their activity. Instead of myocardial hypertrophy, increased cell death and interstitial collagen accumulation become more and

more dominant. Heart failure is characterized by an increased collagen type I deposition. Ventricular remodelling is defined by cardiomyocyte hypertrophy and an extensive myocardial collagen deposition. Transforming growth factor-β (TGFβ)/Smad signalling route seems to be also important in the regulation of cardiac fibrosis. Activation of TGF-β/Smad signalling promotes myofibroblast formation and extracellular matrix (ECM) production, which lead to cardiac fibrosis.

In the failing heart it is crucial to ensure adequate blood supply that follows the growth of the left ventricular hypertrophy. If the rate of angiogenesis is inadequate, the transition to heart failure can occur because of the imbalance between the supply and demand of nutrients and oxygen in the heart.

1.2 The role of mitochondria in cardiac remodelling and heart failure

The primary task of mitochondria is the generation of adenosine triphosphate (ATP) from adenosine diphosphate (ADP) by oxidative phosphorylation, but they also have important roles in ion homeostasis, in several metabolic pathways, in programmed cell death and in ROS production. Oxidative phosphorylation takes place in the inner mitochondrial membrane, where the mitochondrial electron transport chain (ETC) is localised. ETC consists of 4 complexes and these complexes are in charge of mitochondrial respiration and ATP generation, therefore they are indispensable for proper mitochondrial and cellular function. Complex I-III of the respiratory chain are critical for ROS production and therefore mitochondria can become the main source of endogenous ROS production. Mitochondria can generate significant amounts of ROS under several pathologic conditions including hypoxia, mitochondrial hyperpolarization and inhibition of respiratory complexes.

Mitochondria contain their own genome, the mitochondrial DNA (mtDNA), which is a double-stranded circular molecule located in the mitochondrial matrix. During oxidative stress, among others, mitochondrial DNA is damaged, which leads to insufficient ATP generation, deterioration of mitochondrial function and finally to cell death.

Mitochondria are dynamically changing organelles constantly undergoing fusion and fission processes – called as mitochondrial dynamics - that regulate the length, shape, size and number of mitochondria. Mitochondrial fusion is referred to as a process by which the fusion of two mitochondria results in a mitochondrion, in contrast the division of one mitochondrion into two daughter mitochondria is called as mitochondrial fission. Mitochondrial fusion is mediated by GTPases homologues, mitofusins 1 and 2 (MFN1 and MFN2) as well as optic atrophy 1 (OPA1). They regulate the fusion of outer (OMM) and inner mitochondrial membrane (IMM).

Mitochondrial fission is regulated by dynamin-related protein 1 (DRP1), DRP1 is usually localized in the cytosol and translocates to OMM where it is harboured via receptors. DRP1 forms a ring-like structure around the mitochondria what results in the narrowing of the membrane. After that, the hydrolysis of GTP enhances the constriction of membrane and therefore determines the potential future site of mitochondrial fission. DRP1 is controlled by numerous post-translational modifications including

phosphorylation, ubiquitinylation, SUMOylation and nitrosylation. Two main phosphorylation sites in DRP1 have been identified which lead to the modulation of its function. DRP1^{Ser616} phosphorylation activates the translocation of DRP1 to OMM and therefore induces subsequent mitochondrial fragmentation. DRP1^{Ser637} phosphorylation regulated by protein kinase A (PKA) suppresses its translocation to mitochondria and thus inhibits its activity

In addition to mitochondrial dynamics, another very important part of the mitochondrial quality control is the mitochondrial biogenesis as well. Mitochondrial biogenesis can be determined as the growth and division of pre-existing mitochondria, it is accompanied by an increased variation in mitochondria number, size and mass as well. The most important regulatory factor playing a part in the mitochondrial biogenesis is peroxisome proliferator-activated receptor-γ coactivator-1α (PGC-1α), The regulation of PGC-1α can be mediated in several ways.

The mitochondrial network plays a fundamental role in energy metabolism and therefore in maintaining the proper cardiac function. The abnormalities of mitochondrial ultrastructure, dynamics and function altogether lead to a disruption of energy supply and ultimately to the development of heart failure (Fig.2).

The imbalance between fusion and fission processes leads to impaired mitochondrial function. The reduction of fusion process is associated with abnormal cristae morphology, mitochondrial fragmentation and increased apoptosis, while increased fission results in fragmentation of mitochondrial network. In addition to ultrastructural and dynamic changes, functional changes such as reduced ATP production and elevated ROS production are also accompanied by the progression of heart failure.

In heart failure, fission processes predominate, resulting in a fragmented mitochondrial network that is unable to perform its function of providing energy to the cell, thereby inducing cell death. One of the associated phenomena of fission processes is the increased ROS production. These results raised the possibility that mitochondria could be new therapeutic targets in the treatment of heart failure.

Therefore, pharmacological modulation of mitochondrial quality control could have a beneficial effect under cellular stress and in this way could be a novel therapeutic approach in various cardiac diseases characterized by mitochondrial damage induced by oxidative stress. As a result, BGP-15 molecule has become the focus of our attention, which, in addition to its various cytoprotective effects, also promotes mitochondrial fusion.

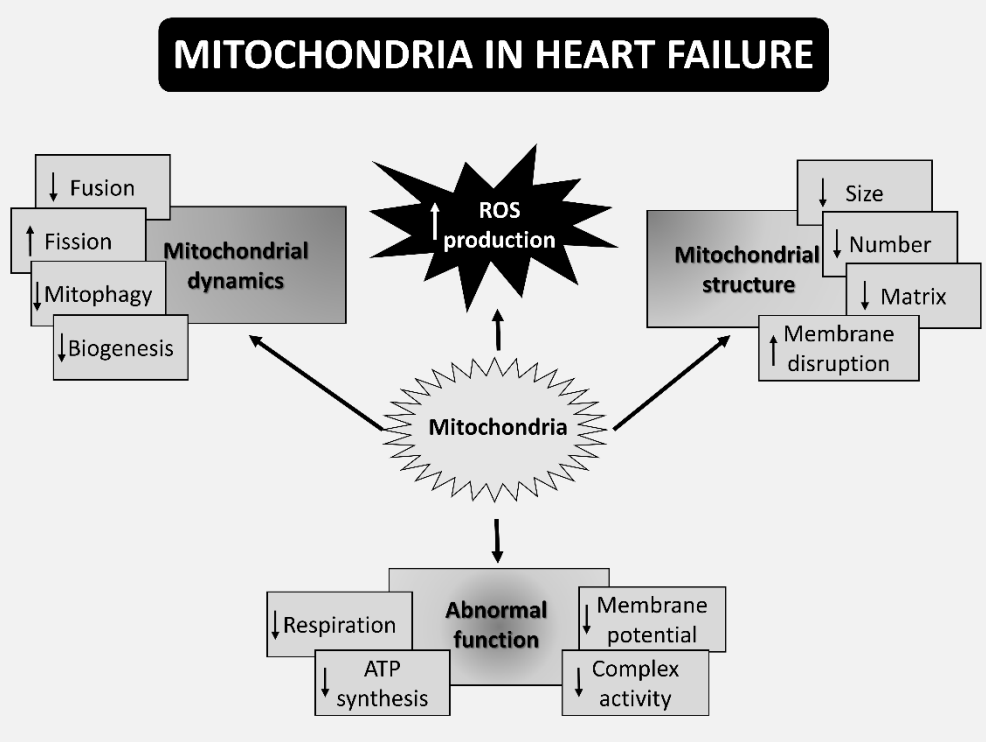

Figure 2. The role of mitochondria in the progression of heart failure

1.3 BGP-15

BGP-15 (C14H22N4O2·2HCl; O-[3-piperidino-2-hydroxy-1-propyl]-nicotinic acid amidoxime dihydrochloride) is a nicotinic amidoxime derivate. BGP-15 protects against oxidative stress during ischemia-reperfusion and is able to reduce the mitochondrial ROS production and to inhibit the poly(ADP-ribose) polymerase-1 (PARP-1) enzyme. BGP-15 also prevents against atrial fibrillation in a transgenic mouse model of heart failure. Furthermore, it has beneficial effects on diastolic dysfunction in a diabetic cardiomyopathy model. Moreover, Szabo et al. demonstrated that BGP-15 protects the lung structure in a model of pulmonary arterial hypertension. More importantly it was the first article to describe that BGP-15 promotes mitochondrial fusion via activating Opa1 protein. Despite these promising results, its specific intracellular target is still unknown and the exact mechanism of action has not been elucidated.

The aim of our study was to investigate the role of BGP-15 in hypertension-induced heart failure. We focused predominantly on factors that regulate the remodelling processes, myocardial fibrosis and the pattern of related signalling pathways. In addition, our goal was to further characterize the mitochondrial effects of BGP-15 in a chronic hypertension induced heart failure animal model and “in vitro” using primer neonatal rat cardiomyocytes (NRCM). We studied the impact of BGP-15 on the processes of mitochondrial quality control, particularly on fusion-fission processes, on mitochondrial biogenesis as well as on mitochondrial function.

2. AIMS OF THE WORK

The aim of our work was to examine the effects of BGP-15 in a chronic hypertension-induced heart failure model and “in vitro” using primer neonatal rat cardiomyocytes (NRCM).

1. Our goal was to study the effect of BGP-15 on structure and function of heart.

2. We aimed to investigate the effects of BGP-15 on signal transduction pathways taking part in the development of cardiac remodelling and heart failure.

3. We aimed to determine its effect on the myocardial fibrotic processes.

4. We examined the effects of BGP-15 on mitochondrial fusion and fission processes as well as on mitochondrial biogenesis.

5. We tried to clarify the role of BGP-15 on mitochondrial function under stress situations.

3. MATERIALS AND METHODS

3.1 Animal model

15-month-old male Wistar Kyoto (WKY) and spontaneously hypertensive rats (Charles River Laboratories, Budapest, Hungary) were used in the experiments. One or two animals were housed per cage under standardized conditions throughout the experiment, with 12h dark-light cycle in solid-bottomed polypropylene cages and received commercial rat chew and water ad libitum. 7 SHRs were sacrificed at the beginning of the experiment as a baseline group (SHR-Baseline). SHRs were randomly divided into two groups: SHR-B and SHR-C. SHR-B group was treated with BGP-15, a water-soluble compound (25 mg/b.w. in kg/day, n=7), while SHR-C group received only placebo (n=7, SHR-C) per os for 18 weeks. BGP-15 was a gift from N-Gene Inc. (New York, NY, USA). Dosage of BGP-15 administered in the drinking water was based on our preliminary data regarding the volume of daily fluid consumption. WKY rats were used as age-matched normotensive controls (n=7). Non-invasive blood pressure measurements were performed on each animal on three occasions at Weeks 0, 9, and 18 of the treatment period. Blood pressure measurements were performed by the non-invasive tail-cuff method as described earlier. At the beginning and at the end of the 18-week-long period, echocardiographic measurements were performed. At the end of the 18 weeks, animals were sacrificed, blood was collected to determine the concentration of plasma brain-derived natriuretic peptide (BNP), then hearts were removed. Atria and great vessels were trimmed from the ventricles and the weight of the ventricles was measured. Hearts were fixed in 10% formalin for histology or freeze-clamped for Western blot analysis. In order to detect the extent of fibrotic areas, histologic samples were stained with Picrosirius red and Collagen type I immunohistochemistry was also made. The phosphorylation state of TGFβ, Smad2 and 3, Akt-1, GSK-3β and MAPK signalling molecules was monitored by Western blotting. In our research, the following group notations were used according to the applied treatment: WKY: age-matched normotensive Wistar-Kyoto rats, SHR-Baseline: 15-month-old spontaneously hypertensive rats before the treatment period, SHR-C: 19-month-old spontaneously hypertensive rats after the 18-week-long placebo treatment, SHR-B: 19-month-old spontaneously hypertensive rats after the 18-week-long treatment period with BGP-15.

3.2 Neonatal rat cardiomyocyte (NRCM) cell culture

Cardiomyocytes were isolated using the Pierce™ Primary Cardiomyocyte Isolation Kit (Life Technologies, Carlsbad, CA, USA #88281) from 1-3-day-old neonatal Wistar rats. NRCMs were cultivated in normal culture conditions, 37°C, saturated humidity atmosphere of 95% air and 5% CO_2. Fresh medium was added every 2-3 days.

On the day of the experiments, cells were washed once in PBS and added fresh medium, then treated with 150 μM H_2O_2 with or without 50 μM BGP-15 for 0.5 hour. The following groups were created according to the applied treatment: Control group: cells without any treatment, BGP-15 group: cells

with only 50 μM BGP-15 for 0.5 hour, H_2O_2 group: cells with 150 μM H_2O_2 for 0.5 hour, H_2O_2+BGP-15 group: cells with 150 μM H_2O_2 and 50 μM BGP-15 for 0.5 hour. Evaluation of mitochondrial fragmentation was measured with fluorescent microscopy. Quantification of mitochondrial DNA (mtDNA) damage was monitored by real-time PCR. The mitochondrial membrane potential was measured with JC-1 assay. Agilent Seahorse Extracellular Flux (XFp) Analyzer (Agilent Technologies, (Santa Clara, CA, USA)) was used to determine the NRCM cells' mitochondrial energy metabolism and function. Citrate synthase actzivity in NRCM cells was measured using a kit from Sigma Aldrich (MAK193) following the manufacturer's instruction.

4. RESULTS

4.1 BGP-15 improved left ventricular function, moderated left ventricular hypertrophy and decreased the heart-failure-induced elevation of plasma BNP level

Table 1. Effect of BGP-15 treatment on echocardiographic parameters

	WKY (n=7)	**SHR-Baseline (n=7)**	**SHR-C (n=7)**	**SHR-B (n=7)**
	Mean ± SEM	**Mean ± SEM**	**Mean ± SEM**	**Mean ± SEM**
Septum	1.93±0.03	2.29±0.07**	2.32 ± 0.07**	2.09 ± 0.08*,§
PW	1.90±0.04	2.06±0.06*	1.97 ± 0.08*	1.81 ± 0.07§
LVIDd (mm)	7.61±0.14	7.75±0.15	8.55 ± 0.23**,##	8.31 ± 0.18**
LVIDs (mm)	4.54±0.13	4.60±0.21	5.87 ± 0.31**,##	5.19 ± 0.32§
LVEDV (µl)	310.25±12.85	323.07±14.59	402.40 ± 24.76**,##	377.19 ± 17.37**
LVESV (µl)	96.01±6.85	101.51±12.27	175.52 ± 22.46**,##	137.23 ± 16.46**,§
LV mass (mg)	1029.81±43.84	1384.42±40.69**	1587.38 ± 106.36**,#	1321.44 ± 75.58*,§
EF%	70.48±1.12	69.59±2.41	57.21 ± 3.02**,##	64.30 ± 2.88*,§
E/E'	30.45±2.00	30.32±2.98	40.41± 2.94**,##	25.71 ± 3.03§§
BNP (pg/ml)	302.76±13.76	325.19±10.89	755.14±33.34*,#	352.04±22.50§

*Septum: thickness of the septum, PW: thickness of the posterior wall, LVIDd: left ventricular (LV) end-diastolic inner diameter, LVIDs: LV end-systolic inner diameter, LVEDV: LV end-diastolic volume, LVESV: LV end-systolic volume, LV mass: calculated weight of left ventricle, EF: ejection fraction, E: mitral peak velocity of early diastolic filling, E': early diastolic mitral annular velocity, BNP: B-type natriuretic peptide. WKY: age-matched normotensive Wistar-Kyoto rats, n=7; SHR-Baseline: 15-month-old spontaneously hypertensive rats, n=7; SHR-C: 19-month-old spontaneously hypertensive rats received placebo for 18 weeks, n=7; SHR-B: 19-month-old spontaneously hypertensive rats received BGP-15 for 18 weeks, n=7. *p<0.05 vs. WKY, **p<0.01 vs. WKY, #p<0.05 vs. SHR-Baseline, ##p<0.01 SHR-Baseline, §p<0.05 vs. SHR-C, §§p<0.01 vs. SHR-C.*

4.2 BGP-15 treatment prevented interstitial collagen deposition and favourably influenced the diameter of cardiomyocytes

Histological staining of the left ventricle of rat hearts was performed with Picrosirius red staining (Fig. 3) and collagen I immunohistochemistry, that were used to monitor the degree of fibrosis. Only a low amount of interstitial collagen could be seen in the WKY group using the Picrosirius red staining (Fig. 3). The extent of fibrosis was significantly higher in the SHR groups compared to the WKY group ($p<0.05$, SHR-Baseline vs. WKY; $p<0.01$, SHR-C and SHR-B vs. WKY). Chronic high blood pressure-induced heart failure caused a further elevation of collagen deposition in SHR-C group ($p<0.01$, vs. SHR-Baseline group). BGP-15 treatment, however, resulted in a significant decrease in the amount of interstitial fibrosis in the SHR-B group compared to non-treated hypertensive animals ($p<0.01$, SHR-B

vs. SHR-C) (WKY: 11.78±1.00%; SHR-Baseline: 16.59±1.03%; SHR-C: 32.42±1.52%; SHR-B: 22.64±1.09%).

Similar observations could be made in the case of type I collagen immunohistochemistry. Only a low amount of interstitial collagen was observed in the WKY group (WKY: 9.15±0.54%; SHR-Baseline: 15.45±0.69%; SHR-C: 31.24±0.77%; SHR-B: 19.92±0.72%), however, in the case of hypertensive groups, even the initial value was higher than in the WKY group ($p<0.01$ vs. SHR-Baseline). This elevation became more pronounced by the end of the treatment period ($p<0.01$ SHR-C vs. WKY, SHR-Baseline groups). Due to BGP-15 treatment the interstitial collagen deposition was significantly decreased in the SHR-B group compared to the SHR-C group ($p<0.01$). It can be concluded that BGP-15 treatment significantly reduced the extent of interstitial fibrosis in the myocardium.

Histological sections from the left ventricle of the heart stained with Picrosirius red were also used to study the cell diameters. The diameter of cardiomyocytes was markedly elevated in SHR groups compared to the WKY group (WKY: 16.02±0.64µm; SHR-Baseline: 22.76±0.70 µm; SHR-C: 33.86±1.82 µm; SHR-B: 28.57±0.57 µm). This difference was the most pronounced in the case of SHR-C ($p<0.01$, SHR-C vs. WKY). BGP-15 treatment resulted in significantly lower cell diameters in the SHR-B group compared to the SHR-C group ($p<0.01$; SHR-B vs. SHR-C).

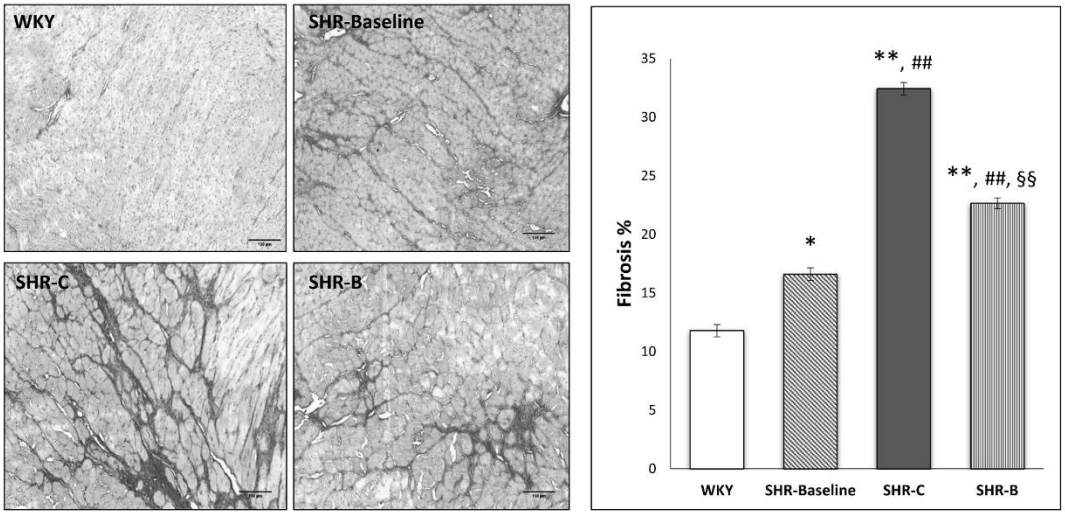

Figure 3. Effect of BGP-15 treatment on the extent of interstitial fibrosis, on the type I collagen deposition and on the diameter of cardiomyocytes. *Representative histological sections stained with Picrosirius red (n=7). Scale bar: 150 µm, magnification: 10-fold. Densitometric evaluation of the sections is shown * $p<0.05$ vs. WKY, ** $p<0.01$ vs. WKY, ##$p<0.01$ vs. SHR-Baseline, §§$p<0.01$ vs. SHR-C. WKY: age-matched normotensive Wistar-Kyoto rats; SHR-Baseline: 15-month-old spontaneously hypertensive rats; SHR-C: 19-month-old spontaneously hypertensive rats received placebo for 18 weeks; SHR-B: 19-month-old spontaneously hypertensive rats received BGP-15 for 18 weeks.*

4.3 BGP-15 treatment favourably influenced the TGF-β/SMAD signalling pathway

The level of TGF-β was significantly elevated in all hypertensive groups compared to the WKY group ($p<0.05$, SHR-B vs. WKY, $p<0.01$ SHR-Baseline, SHR-C vs. WKY). In case of SHR-C group a further increasing tendency could be seen by the end of the treatment period compared to the baseline values (NS). However, BGP-15 treatment caused a significant decrease in the TGF-β level compared to the untreated SHR animals ($p<0.01$, SHR-B vs. SHR-C), moreover TGF-β level in this group was even lower than in the SHR-Baseline group ($p<0.05$, SHR-B vs. SHR-Baseline). In the case of Smad2 phosphorylation we observed a mild increase in the SHR-Baseline group compared to the WKY group, however this elevation was not significant. The phosphorylation of $Smad2^{Ser465/467}$ was significantly increased in the SHR-C animals compared to the WKY and Baseline Groups ($p<0.05$). BGP-15 treatment resulted in a significant reduction in the phosphorylation level of $Smad2^{Ser465/467}$ in the treated group ($p<0.01$ SHR-B vs. SHR-C). There were no significant differences regarding the phosphorylation of $Smad3^{Ser423/425}$ between the groups.

4.4 BGP-15 favourably affected the phosphorylation of Akt-1Ser473 and GSK-3βSer9

The level of Akt-1^{Ser473} phosphorylation was moderate both in the WKY group and in the SHR-Baseline group. In the SHR-C group, phosphorylation of Akt-1^{Ser473} was slightly, but significantly increased ($p<0.01$ SHR-C vs. WKY and SHR-Baseline groups). However, BGP-15 treatment caused a marked increase in the Akt-1^{Ser473} phosphorylation in SHR-B animals ($p<0.01$ SHR-B vs. SHR-C group).
The phosphorylation level of GSK-$3\beta^{Ser9}$ was low in the WKY group similarly to Akt-1^{Ser473} phosphorylation. In the SHR-Baseline and the SHR-C groups, however, slightly but not significantly elevated phosphorylation could be seen. The highest phosphorylation of GSK-$3\beta^{Ser9}$ was measured in the SHR-B group. This elevation was highly significant comparing to other SHR groups ($p<0.05$ SHR-B vs. SHR-C, $p<0.01$, SHR-B vs. SHR-Baseline group).

4.5 BGP-15 decreased the activity of MAPKs

The level of MKP-1 protein was low in the WKY and SHR-Baseline groups, however, a significant increase was observed in the SHR-C group ($p<0.01$, SHR-C vs. WKY as well as in the SHR-Baseline groups). The amount of MKP-1 protein increased further in the SHR-B group as a result of the BGP-15 treatment ($p<0.01$, SHR-B vs. SHR-C). The level of Erk1/$2^{Thr202/Tyr204}$ phosphorylation was less pronounced in the SHR-C group compared to the WKY group and to the baseline level ($p<0.05$, SHR-C vs. WKY). BGP-15 treatment, however, caused a significant elevation in the phosphorylation of Erk1/$2^{Thr202/Tyr204}$ compared to the SHR-C group ($p<0.01$, SHR-B vs. SHR-C). The level of p38-$MAPK^{Thr180/Tyr182}$ and $JNK^{Thr183/Tyr185}$ phosphorylation was low in the WKY and in the SHR-Baseline groups. The highest phosphorylation level of p38-$MAPK^{Thr180/Tyr182}$ and $JNK^{Thr183/Tyr185}$ could be seen in the SHR-C animals ($p<0.01$, SHR-C vs. WKY and SHR-Baseline). BGP-15 treatment reduced this

phosphorylation of p38-MAPK$^{Thr180/Tyr182}$ and JNK$^{Thr183/Tyr185,}$ too and this reduce was significant in the case of JNK$^{Thr183/Tyr185}$ compared to the SHR-C group ($p<0.01$).

4.6 BGP-15 improved the mitochondrial ultrastructure in a hypertension-induced heart failure animal model

Longitudinal sections of myocardium were evaluated to assess the morphology of interfibrillar mitochondria (IFM) by electron microscopy. The mitochondria of SHR-C rats differ from the normal mitochondria of WKY rats, because they are morphologically more heterogeneous (n = 5 from each group, 3–5 block from each animal). In the non-treated hypertensive animals (SHR-C), mitochondria were loosely arranged between the contractile elements. Moreover, in the SHR-C group extensive disruption of mitochondrial cristae and enlarged intracristal spaces could be observed. Their shape was often elongated, and the mitochondrial matrix was very light. The mitochondrial ultrastructure in the SHR-B group was similar to that of WKY rats. In treated SHR animals (SHR-B) normal, large and less elongated mitochondria with tightly packed cristae and electron-dense matrix was seen.

The area of IFM was assessed on electron micrographs (~500 mitochondria/group were measured; Fig. 11 b). We assessed relative frequencies of the measured mitochondrial areas in arbitrary intervals of 0.3 μm^2 (Fig. 4).

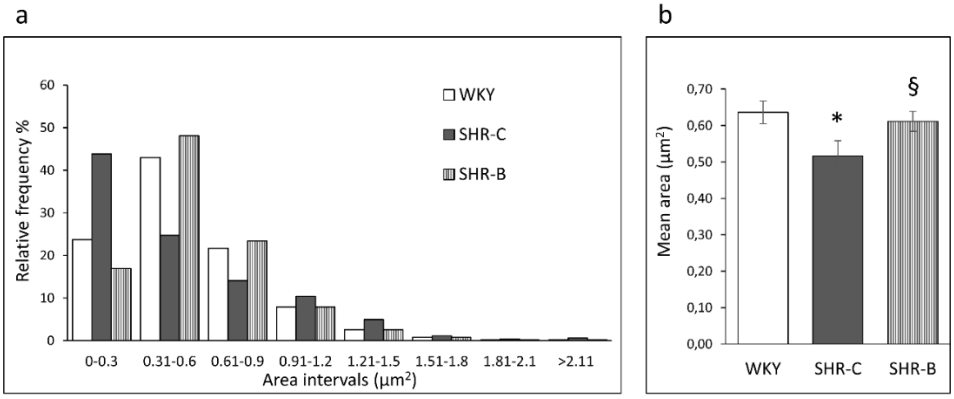

Figure 4. Heart failure-induced fragmentation of interfibrillar mitochondria in the myocardium. *(a) Relative frequencies of measured mitochondrial areas in each arbitrary area interval. (b) Means of area values in the given groups (~500 mitochondria/group). WKY: age-matched normotensive Wistar-Kyoto rats, SHR-C: non-treated spontaneously hypertensive rats, SHR-B: spontaneously hypertensive rats receiving BGP-15 for 18 weeks. Data are expressed as mean±SEM. *p<0.05 vs. WKY, §p<0.05 vs. SHR-C).*

4.7 BGP-15 increased the expression level of mitochondrial fusion proteins and decreased the expression level of mitochondrial fission proteins in SHR animals

Regarding the mitochondrial fusion proteins, we determined the levels of OPA1, MFN1 and MFN2 in the myocardium using Western blot analysis. We observed that the level of OPA1 was moderately decreased in the SHR-C group compared to the WKY group ($p<0.05$, SHR-C vs. WKY). However,

BGP-15 treatment caused a significant elevation of OPA1 level in the SHR-B group ($p<0.01$ SHR-B vs. WKY, $p<0.05$ SHR-B vs. SHR-C). Considering the amount of MFN1 protein level, there was a significant increase in hypertensive animals by the end of the study compared to the baseline levels ($p<0.05$, SHR-C and SHR-B vs. SHR-Baseline), however, there was no difference between the SHR groups. The level of MFN2 protein was moderately lower in the SHR-C group than in the WKY group ($p<0.05$), and very similar changes could be seen in the case of OPA1. In the SHR-B group these parameters significantly increased due to the BGP-15 treatment compared to the other groups ($p<0.01$ SHR-B vs. WKY, SHR-C).

The myocardial concentration of fission proteins Fis1 and DRP1 were determined in both total and fractionated Western blot samples. The level of Fis1 increased in the SHR-C group compared to the WKY group ($p<0.05$, SHR-C vs. WKY). This elevation was, however, significantly diminished due to BGP-15 treatment ($p<0.05$ SHR-B vs. SHR-C). In the case of the fission protein DRP1, the total level was significantly decreased due to BGP-15 treatment compared to other groups ($p<0.01$ SHR-B vs. WKY, SHR-C). The phosphorylation level of DRP1 at the Ser616 and Ser637 residues was also measured. The phosphorylation of $DRP1^{Ser616}$ and $DRP1^{Ser637}$ was moderate in the WKY group. In the SHR-C group, however, phosphorylation of $DRP1^{Ser616}$ was significantly higher ($p<0.01$ vs. WKY and SHR-Baseline). BGP-15 treatment on the other hand decreased the $DRP1^{Ser616}$ phosphorylation in SHR-B animals ($p<0.01$ vs. SHR-C group). Regarding the phosphorylation level of $DRP1^{Ser637}$, we observed a significant increase in the SHR-C group ($p<0.01$ vs. WKY, SHR-Baseline). Moreover, BGP-15 treatment caused a further increase in the $DRP1^{Ser637}$ phosphorylation in SHR-B animals ($p<0.01$ SHR-B vs. SHR-C).

The intracellular distribution of DRP1 was also measured. We observed that the DRP1 accumulated in the mitochondrial fractions of SHR-C animals compared to normotensive animals ($p<0.01$, SHR-C vs. WKY). BGP-15 treatment resulted in a significantly reduced translocation of DRP1 into the mitochondria ($p<0.01$ vs. SHR-C), thereby preserving it in a higher concentration in the cytosolic fraction.

4.8 BGP-15 enhanced the mitochondrial biogenesis in SHR animals

There were no significant differences between the WKY, SHR-Baseline and SHR-C groups regarding the PGC-1α level. However, BGP-15 treatment caused a significant increase in the amount of PGC-1α compared to the non-treated hypertensive animals ($p<0.01$, SHR-B vs. SHR-Baseline and SHR-C group). In the case of $AMPK^{Thr172}$ phosphorylation a significant increase was observed in the SHR-C group compared to the SHR-Baseline group ($p<0.01$, SHR-C vs. SHR-Baseline). BGP-15 treatment significantly reduced the phosphorylation of $AMPK^{Thr172}$ compared to the SHR-C group ($p<0.01$ SHR-B vs. SHR-C). The $CREB^{Ser133}$ phosphorylation was modest in the WKY group similarly to the phosphorylation of $AMPK^{Thr172}$. There was significant increase in the phosphorylation level of $CREB^{Ser133}$ in the SHR-C group compared to the baseline value and to the normotensive animals ($p<0.01$,

SHR-C vs. WKY). Moreover, BGP-15 treatment caused a further increase in the $CREB^{Ser133}$ phosphorylation compared to non-treated SHR animals ($p<0.05$ SHR-B vs. SHR-C group) and to the baseline value ($p<0.01$ SHR-B vs. SHR-Baseline). The highest VDAC protein level was observed in the WKY group. This level was significantly lower in the hypertensive groups ($p<0.01$ WKY vs. SHR-Baseline, SHR-C and SHR-B). By the end of the treatment period VDAC became higher compared to the initial value ($p<0.01$, SHR-C vs. SHR-Baseline). Further significant increase was seen in the SHR-B group ($p<0.05$ SHR-B vs. SHR-C).

4.9 Effect of BGP-15 administration on mitochondrial morphology of NRCM cells

To examine the changes of the mitochondrial network we used the MitoTracker Red CMXRos staining method. BGP-15 per se had no effect on the complexity of the mitochondrial network. Filamentous mitochondrial network was observed in the Control group, H_2O_2 treatment, however, caused a marked injury to the mitochondrial network. As a result of the H_2O_2 induced fission processes, degradation of the mitochondrial network could be observed, which led to mitochondrial fragmentation. BGP-15 treatment prevented the mitochondrial network from the oxidative stress-induced fragmentation and preserved the normal filamentous network of mitochondria.

4.10 BGP-15 treatment increased the level of fusion proteins and reduced the mitochondrial fission proteins level in NRCMs

We assessed the levels of OPA1, MFN1 and MFN2 proteins in total Western blot samples of NRCM cells. BGP-15 treatment per se had no effect on the amount of these parameters in the non-stressed cells in compared to the Control group. H_2O_2 treatment caused a slight decrease in the level of MFN1 and MFN2 proteins and a slight increase in the level of OPA1, but these changes were not significant. However, BGP-15 treatment caused a significant increase in the amount of OPA1, MFN1 and MFN2 proteins in H_2O_2 stressed cells compared to the untreated H_2O_2-stressed group ($p<0.05$ H_2O_2-BGP15 vs. H_2O_2).

We determined the levels of Fis1 and DRP1 in total and in fractionated Western blot samples in NRCM cells. No significant difference was found in non-stressed cells due to BGP-15 compared to the Control group. The level of Fis1 increased markedly in the H_2O_2 group compared to the Control group ($p<0.01$, H_2O_2 vs. Control). BGP-15 treatment blunted this change ($p<0.05$, H_2O_2-BGP15 vs. H_2O_2 group). In the case of the total level of the fission mediator DRP1 protein, that was a significant elevation in the H_2O_2 group due to oxidative stress ($p<0.05$ H_2O_2 vs. Control group). However, a control-like value could be seen in the treated group compared to the H_2O_2 group ($p<0.05$ H_2O_2-BGP15 vs. H_2O_2 group). The phosphorylation of DRP1 on Ser616 and Ser637 residues was also evaluated. The phosphorylation of both DRP1 phospho-form was moderate in the Control group. Phosphorylation of $DRP1^{Ser616}$ considerably increased in the H_2O_2 group ($p<0.05$ H_2O_2 vs. Control group). However, BGP-15 treatment

decreased DRP1^{Ser616} phosphorylation compared to non-treated stressed cells ($p<0.05$ H_2O_2-BGP-15 vs. H_2O_2 group). Measuring the phosphorylation level of DRP1^{Ser637}, a significant decrease could be observed in the H_2O_2 group compared to the Control group ($p<0.01$ H_2O_2 vs. Control group). However, BGP-15 treatment remarkably enhanced the DRP1^{Ser637} phosphorylation ($p<0.01$ H_2O_2-BGP15 vs. H_2O_2 group).

Finally, the intracellular distribution of the fission mediator DRP1 protein was examined. Significantly higher portion of DRP1 could be found in the mitochondrial fraction of cells in the H_2O_2 group compared to the BGP-15 treated group. The translocation of DRP1 protein from the cytosol to the mitochondria was decreased due to BGP-15 treatment and in this way it resulted in higher levels of DRP1 in the cytosolic fraction and lower concentration in the mitochondrial fraction ($p<0.01$ vs. H_2O_2 group).

4.11 BGP-15 favourably influenced the regulation of mitochondrial biogenesis in NRCMs

We determined the levels of PGC-1α, CREB and VDAC in the total Western blot samples of NRCMs. BGP-15 treatment had no effect on these factors in non-stressed cells compared to the Control group. The PGC-1α level was increased in the H_2O_2 group compared to the Control group ($p<0.01$ vs. Control). However, this elevation was much more marked in the treated group ($p<0.01$ H_2O_2-BGP15 vs. Control and H_2O_2 groups). The phosphorylation level of CREB^{Ser133} was low in the Control group. However, a significant increase was seen in the phosphorylation level of CREB^{Ser133} in the H_2O_2 group ($p<0.01$ H_2O_2 vs. Control). BGP-15 treatment further increased the phosphorylation level of CREB^{Ser133} ($p<0.01$, H_2O_2-BGP15 vs. H_2O_2 group). The level of VDAC was slightly decreased in the H_2O_2 group compared to the Control group ($p<0.05$ H_2O_2 vs. Control). However, it was significantly elevated in the BGP-15 treated group ($p<0.01$ H_2O_2-BGP-15 vs. H_2O_2 group).

Moreover, we investigated mitochondrial DNA content compared to the nuclear DNA. The relative mitochondrial DNA content was determined by "real-time" PCR, using COX1 and COX3 primers, normalized to a nuclear-encoded β-actin gene. We found that BGP-15 treatment increased the relative expression levels of COXI and COXIII genes compared to the H_2O_2 group ($p<0.05$ H_2O_2-BGP-15 vs. H_2O_2 group).

Furthermore, we also performed a widely used method for studying mitochondrial biogenesis by measuring the activity of citrate synthase. Citrate synthase activity was reduced in hydrogen-peroxide stressed group compared to control group ($p<0.01$ H_2O_2 vs. Control). The citrate synthase activity was increased significantly due to the treatment ($p<0.01$ H_2O_2-BGP-15 vs. H_2O_2 group).

Finally, we measured the level of NDUFs1 subunit of NADH-ubiquinone oxidoreductase and UQCRC1 subunit of Ubiquinol Cytochrome c Reductase proteins in order to support our finding regarding the effect of BGP-15 on mitochondrial biogenesis. The expression level of NDUFs1 was significantly decreased in the H_2O_2 group ($p<0.01$ H_2O_2 vs. Control). Similar observation was made in the case of UQCRC1 ($p<0.05$ H_2O_2 vs. Control). However, BGP-15 treatment not only protected against the

decrease but also significantly increased the amount of NDUFs1 and UQCRC1 proteins ($p<0.01$ H_2O_2-BGP-15 vs. H_2O_2 group).

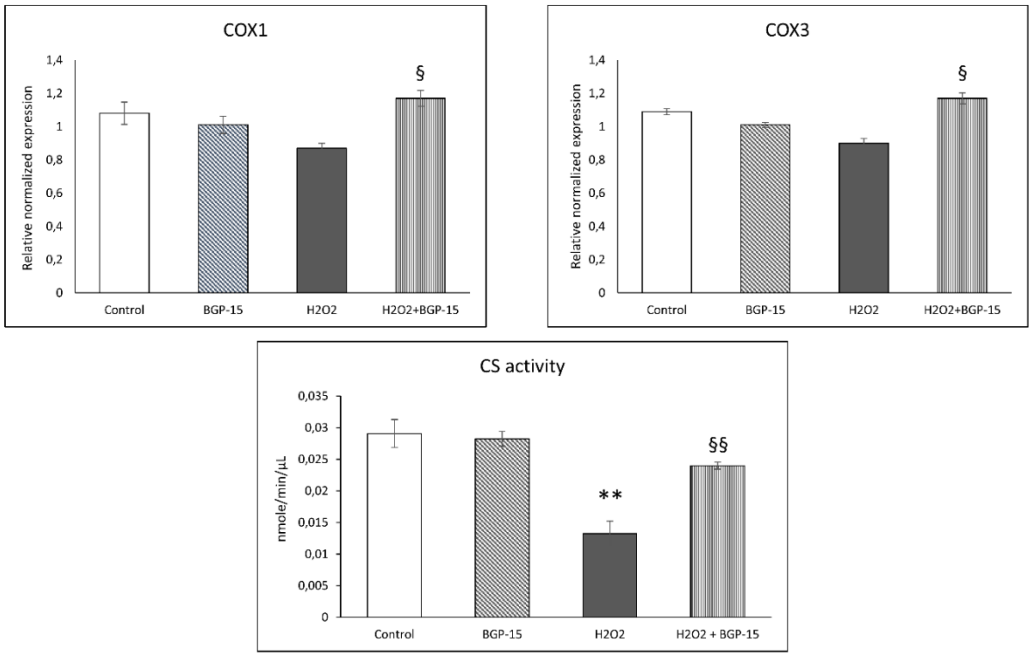

Figure 21. Effect of BGP-15 treatment on the relative DNA content and citrate synthase activity. *Relative expression level of electron transport chain complex IV genes (COXI and COXIII) are presented. Comparison of citrate synthase activity in NRCM cells. Control group: cells without any treatment, BGP-15 group: cells with only 50 µM BGP-15 for 0.5 hour, H_2O_2 group: cells with 150 µM H_2O_2 for 0.5 hour, H_2O_2+BGP-15 group: cells with 150 µM H_2O_2 and 50 µM BGP-15 for 0.5 hour. Values are mean±SEM (n=4). **p<0.01 vs. Control, §§p<0.01 vs H_2O_2 group.*

4.12 BGP-15 treatment protected mitochondrial genome integrity against the ROS-induced damage

Real time detection of long-range polymerase chain reaction (LRPCR) was used to examine the impact of H_2O_2-induced oxidative injury on mtDNA. No significant difference was found with BGP-15 treatment alone compared to the Control group. H_2O_2 induced a significant damage of the mtDNA ($p<0.05$, H_2O_2 vs. Control), the amplification rate of the entire mitochondrial genome was markedly diminished. This unfavourable damage was significantly reduced by BGP-15 treatment ($p<0.01$, H_2O_2-BGP15 vs. H_2O_2).

4.13 Effect of BGP-15 on mitochondrial membrane potential (ΔΨ) and on mitochondrial oxygen consumption and energy metabolism in NRCM cells under oxidative stress

We examined the effect of BGP-15 on mitochondrial membrane potential using JC-1, a cell-permeable voltage-sensitive fluorescent mitochondrial dye. JC-1 emits red fluorescence if the mitochondrial membrane potential is high (aggregated dye), while depolarized mitochondria emit green fluorescence (monomer dye). In the control cells fluorescence microscopy showed strong red fluorescence and weak

green fluorescence, what indicates a high ΔΨm in mitochondria. BGP-15 per se had no effect on mitochondrial membrane potential. The addition of H_2O_2 to cells facilitates the depolarization of mitochondria, resulting in weaker red fluorescence and stronger green fluorescence ($p<0.01$ H_2O_2 vs. Control). If BGP-15 was also administered in peroxide-stressed NRCM cells, the intensity of red fluorescence increased and green fluorescence decreased compared to the H_2O_2 treated cells ($p<0.01$, H_2O_2-BGP15 vs. H_2O_2). Therefore, the quantitative assessment revealed that BGP-15 treatment reduced the H_2O_2-induced depolarization of the mitochondrial membrane, the ΔΨm was similar to that of the Control cells.

To determine the mitochondrial energy metabolism and respiratory function, we used the Agilent Seahorse XFp Analyzer system and the Agilent Seahorse XFp Cell Mito Stress Test (Fig. 6).

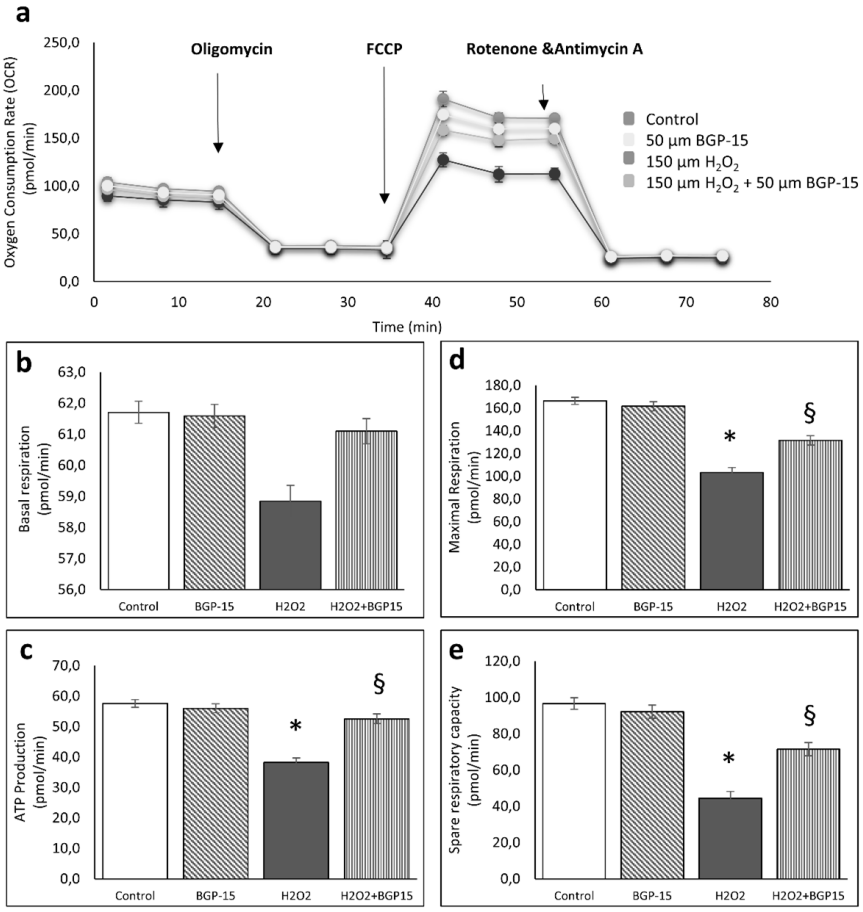

Figure 6. Effect of BGP-15 on mitochondrial oxygen consumption and energy metabolism in NRCM cells, as determined by Agilent Seahorse XFp. *Mitochondrial energy metabolism was measured using a Seahorse XFp analyser. During testing, NRCMs cells were treated with 10 µM oligomycin, 10 µM FCCP, and 5 µM rotenone/antimycin A. Data were automatically calculated according to the Agilent Seahorse XF Cell Mito Stress Test Report Generator. (A) Oxygen consumption rate (OCR). (B) basal respiration. (C) ATP production. (D) maximal respiration. (E) spare respiratory capacity. Control group: cells without any treatment, BGP-15 group: cells with only 50 µM BGP-15 for 0.5 hour, H_2O_2 group: cells with 150 µM H_2O_2 for 0.5 hour, H_2O_2+BGP-15 group: cells with 150 µM H_2O_2 and 50 µM BGP-15 for 0.5 hour. Values are mean±SEM (n=4). *p<0.05 vs. Control, §p<0.05 vs. H_2O_2 group.*

5. DISCUSSION

In this work we aimed to examine the cardio protective effect of BGP-15 in chronic hypertension induced heart failure. Furthermore, we aimed to clarify the effect of BGP-15 on various processes of mitochondrial quality control in a hypertension-induced heart failure model and in vitro using hydrogen peroxide-induced oxidative stress.

The major findings of this study are that BGP-15 has positive effects on cardiac function and structure by inhibiting profibrotic signalling factors and therefore the remodelling itself in an animal model of hypertension-induced heart failure. This cardio protective effect can also be attributable to the mitochondrial effects of BGP-15. BGP-15, besides its mitochondrial fusion promoting effect, also inhibits factors playing part in the mitochondrial fission and enhances their de novo biogenesis under stress situations. As a result of these effects, BGP-15 preserves mitochondrial structure and energy production during hydrogen peroxide-induced oxidative stress as well as in an in vivo heart failure model (Fig.7).

Moreover, our study is the first to demonstrate that BGP-15 preserved the mitochondrial ultrastructure by increased mitochondrial fusion and decreased fission processes and positively affected the translocation processes in chronic hypertension-induced heart failure animal model. Similar changes were seen in the case of fusion and fission processes in NRCM cell culture compared to in vivo model. Furthermore, BGP-15 treatment preserved the mitochondrial membrane potential and improved the mitochondrial function. BGP-15 protected the integrity of the mitochondrial genome and enhanced the de novo biogenesis of mitochondria during hydrogen peroxide-induced oxidative stress. Nevertheless, the exact molecular mechanism of the effects is still unknown, but there are clear evidences regarding the specific mechanism how to BGP-15 acts at important integrator points of signal transduction in certain pathological processes. In order to elucidate the potential underlying molecular mechanisms, further targeted studies should be performed in the future.

Our results revealed that pharmacological modulation of the mitochondrial dynamics under cellular stress could be a novel therapeutic approach in various cardiac diseases characterized by oxidative stress-induced mitochondrial damage.

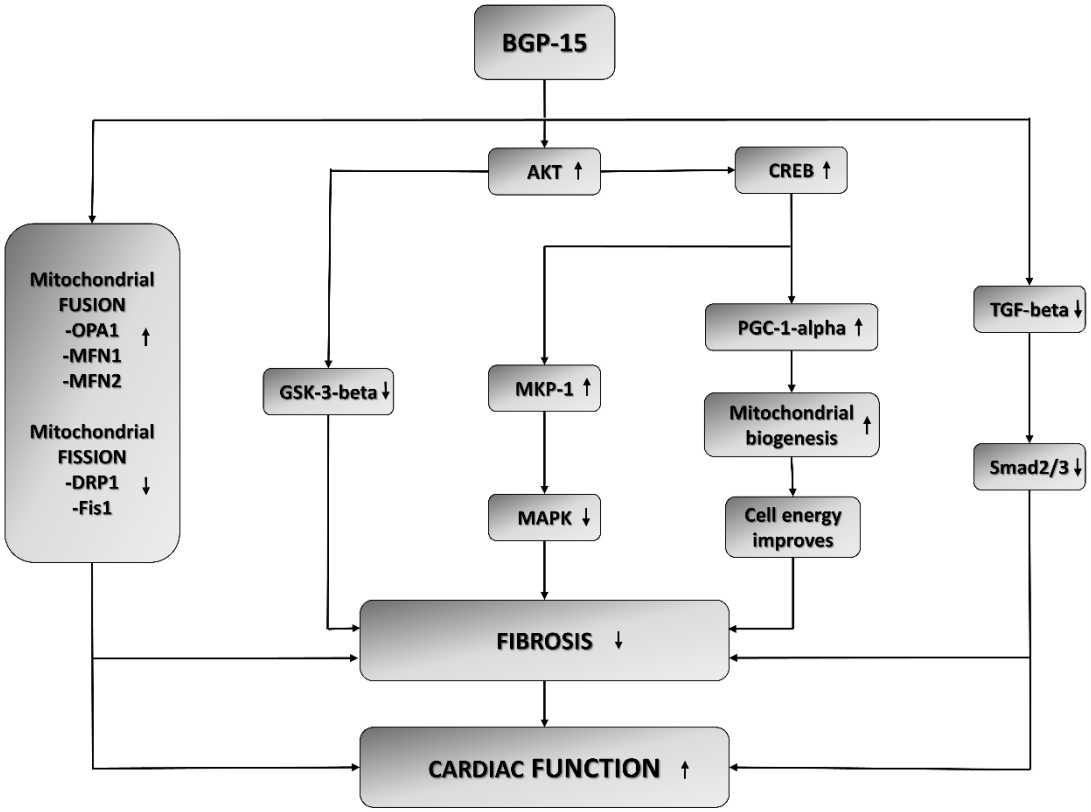

Figure 7. The suspected mechanism of BGP-15 treatment in a hypertension-induced heart failure model. *BGP-15 has beneficial effect against hypertension induced cardiac remodelling and cardiac fibrosis. BGP-15 treatment decreases the activity of TGFβ/Smad and MAPKs signalling factors and in this way it prevents against hypertension induced interstitial collagen deposition. BGP-15 favourably influences the pro-survival signalling pathways. Moreover, the mitochondrial biogenesis is activated due to BGP-15 administration, thereby resulting in an increase in mitochondrial mass. BGP-15 increases the expression level of fusion mediators OPA1 and MFN1/2, moreover decreases the expression level of fission mediators DRP1 and Fis1.*

6. SUMMARY OF THE NEW FINDINGS

1. **The effect of BGP-15 on structure and function of heart.**
   Our research group verified the first time that BGP-15 treatment has beneficial effects on cardiac function in hypertension-induced heart failure.

2. **The effects of BGP-15 on signal transduction pathways taking part in the development of cardiac remodelling and heart failure.**
   BGP-15 treatment beneficially influences the activity of signalling pathways involved in remodelling (Akt/GSK-3β, ERK1/2, JNK, p38 MAPK).

3. **The effect of BGP-15 on the myocardial fibrotic processes.**
   BGP-15 protects against the interstitial collagen deposition via favourable effect on TGF-β/Smad pathway.

4. **The effects of BGP-15 on mitochondrial fusion and fission processes as well as on mitochondrial biogenesis.**
   - BGP-15 prevents mitochondrial ultrastructure against ROS-induced mitochondrial fragmentation.
   - BGP-15 increases the expression level of fusion mediators OPA1 and MFN1/2, moreover decreases the expression level of fission mediators DRP1 and Fis1 in the animal model of heart failure.
   - Mitochondrial biogenesis is enhanced due to BGP-15 treatment in heart failure.
   - BGP-15 preserves the mitochondrial network against oxidative stress-induced mitochondrial fragmentation.
   - BGP-15 increases the expression level of fusion mediators OPA1 and MFN1/2, moreover decreases the expression level of fission mediators DRP1 and Fis1 in NRCMs cell culture in oxidative stress scenarios.
   - Mitochondrial biogenesis increases under hydrogen-peroxide-induced oxidative stress in treated NRCMs cells as a result of BGP-15 treatment.
   - BGP-15 protects against oxidative stress-induced mitochondrial DNA damage.

5. **The role of BGP-15 on mitochondrial function under stress situations.**
   BGP-15 treatment preserves the mitochondrial membrane potential and improves mitochondrial function.

7. ACKNOWLEDGEMENT

These studies were carried out at the 1st Department of Medicine and Department of Biochemistry and Medical Chemistry, Medical School of the University of Pecs between 2017 and 2021.

I would like to express my thanks to my program leader, Professor Kálmán Tóth, who gave me support and useful advice during my work.

I would like to express my deepest appreciation to my project leaders Professor Róbert Halmosi and Dr. László Deres for guiding my studies throughout the field of cardiovascular sciences and providing the possibility of the current work. Without their fundamental guidance and persistent help this dissertation would not have been possible.

I am extremely grateful to Professor Balázs Sümegi (†), who was an extraordinary mentor and taught me a biochemical way of thinking.

My colleagues, Dr. Krisztián Erős, Katalin Ördög and Dr. Kitti Bruszt gave also a hand with the experiments.

I am grateful to Tímea Dózsa, József Nyirádi and Heléna Halász, who provided considerable assistance in the laboratory work throughout my studies.

I express my special thanks to my close friends for their encouraging support and their immense patience during my work.

It is my privilege to thank to my family for their love, caring and sacrifices for educating and preparing me for my future life. I am grateful to them for trusting me in the most difficult times and for encouraging me despite all the difficulties.

8. PUBLICATIONS OF THE AUTHOR

8.1 Relevant publications

HORVATH O, ORDOG K, BRUSZT K, KALMAN N, KOVACS D, RADNAI B, GALLYAS F, TOTH K, HALMOSI R, DERES L. Modulation of mitochondrial quality control processes by BGP-15 in oxidative stress scenarios: from cell culture to heart failure.
Oxidative Medicine and Cellular Longevity 2021 Paper: 6643871, 22 p. (2021)
IF: 6,543

HORVATH O, ORDOG K, BRUSZT K, DERES L, GALLYAS F, SUMEGI B, TOTH K, HALMOSI R. BGP-15 protects against heart failure by enhanced mitochondrial biogenesis and decreased fibrotic remodelling in spontaneously hypertensive rats.
Oxidative Medicine and Cellular Longevity 2021 Paper: 1250858, 13 p. (2021)
IF: 6,543

8.2 Additional publications

ORDOG K, HORVATH O, EROS K, BRUSZT K, TOTH SZ, KOVACS D, KALMAN N, RADNAI B, DERES L, GALLYAS F, TOTH K, HALMOSI R. Mitochondrial protective effects of PARP-inhibition in hypertension-induced myocardial remodeling and in stressed cardiomyocytes.
Life Sciences 268 Paper: 118936, 15 p. (2021)
IF: 5,037

GAL R, DERES L, HORVATH O, EROS K, SANDOR B, URBAN P, SOOS SZ, MARTON ZS, SUMEGI B, TOTH K, HABON T, HALMOSI R. Resveratrol improves heart function by moderating inflammatory processes in patients with systolic heart failure.
Antioxidants 9: 11 Paper: 1108, 19 p. (2020)
IF: 6,312

DERES L, EROS K, HORVATH O, BENCZE N, CSEKO CS, FARKAS S, SERESS L, TOTH K, HALMOSI R. The effects of bradykinin B1 Receptor antagonism on the myocardial and vascular consequences of hypertension in SHR rats.
FRONTIERS IN PHYSIOLOGY 10 Paper: 624, 14 p. (2019)
IF: 3,201

VARADI O, HORVATH O, MARCSIK A, MOLNAR E, PALFI GY, BERECZKI ZS.
Különleges formájú jelképes trepanációk a Dél-Alföldről.
Anthropologiai Közlemények 56 pp. 91-104, 14 p. (2015)

8.3Published abstracts

HORVATH O, DERES L, ORDOG K, BRUSZT K, SUMEGI B, TOTH K, HALMOSI R.
Role of BGP-15 treatment in hypertensive heart failure Progression and mitochondrial protection.
EUROPEAN HEART JOURNAL 40: Suppl. 1 Paper: P5994 (2019)

HALMOSI R, GAL R, DERES L, HORVATH O, MARTON ZS, SUMEGI B, TOTH K, HABON T.
Resveratrol improves cardiac function and exerts an anti-inflammatory effect in systolic heart failure patients.
EUROPEAN HEART JOURNAL 40: Suppl. 1 Paper: P781 (2019)

HORVATH O, ORDOG K, BRUSZT K, DERES L, SUMEGI B, TOTH K, HALMOSI R.
A BGP-15 kezelés hatása a mitokondriális dinamikára és funkcióra élő állat modellen és sejtkultúrában.
CARDIOLOGIA HUNGARICA 49: Suppl. B Paper: B23 (2019)

ORDOG K, HORVATH O, BRUSZT K, HALMOSI R, TOTH K, SUMEGI B, DERES L.
Az L-2286 kezelés hatása oxidatív stresszben a mitokondriális dinamikára és funkcióra in vitro kardiomioblaszt modellben.
CARDIOLOGIA HUNGARICA 49: Suppl. B Paper: B14 (2019)

HORVATH O, DERES L, EROS K, ORDOG K, HABON T, SUMEGI B, TOTH K, HALMOSI R.
Oxidatív stressz indukálta változások a szívizomsejtek mitokondriális dinamikájára sejtes modellekben.
CARDIOLOGIA HUNGARICA 48: Suppl. C Paper: C38 (2018)

ORDOG K, DERES L, EROS K, HORVATH O, HABON T, SUMEGI B, TOTH K, HALMOSI R.
A BGP-15 kezelés hatása a hipertenzió indukált kardiális remodellingrein vivo SHR modellben.
CARDIOLOGIA HUNGARICA 48: Suppl. C Paper: C34 (2018)

GAL R, DERES L, HORVATH O, PRAKSCH D, MARTON ZS, SUMEGI B, TOTH K, HABON T, HALMOSI R.
A rezveratrol hatása a non-invazív klinikai kardiológiai és laboratóriumi paraméterekre szisztolés típusú szívelégtelenségben.
CARDIOLOGIA HUNGARICA 48: Suppl. C Paper: C65 (2018)

HORVATH O, DERES L, EROS K, ORDOG K, HABON T, SUMEGI B, TOTH K, HALMOSI R.
Oxidative stress-induced changes in mitochondrial dynamics of cardiomyocytes in cell culture.
EUROPEAN JOURNAL OF HEART FAILURE 20: Suppl. 1 pp. 616-616. Paper: P2281, 1 p. (2018)

ORDOG K, DERES L, EROS K, HORVATH O, HABON T, SUMEGI B, TOTH K, HALMOSI R.
Effect of BGP-15 treatment on hypertension induced cardiac remodeling in an in vivo SHR model.
EUROPEAN JOURNAL OF HEART FAILURE 20: Suppl. 1 pp. 515-515. Paper: P1975, 1 p. (2018)

HALMOSI R, GAL R, DERES L, HORVATH O, PRAKSCH D, MARTON ZS, SUMEGI B, TOTH K, HABON T.
The effect of resveratrol on non-invasive cardiologic and laboratory parameters in systolic heart failure.
EUROPEAN JOURNAL OF HEART FAILURE 20: Suppl. 1 pp. 565-565. Paper: P2133, 1 p. (2018)

HORVATH O.
A paraoxonáz aktivitás, a totál oxidáns státusz és a lipid profil alakulása különböző kardiovaszkuláris rizikócsoportba tartozó egyénekben.
Érbetegségek, XXIII. évfolyam 2. szám, 2016/2

BERECZKI ZS, VARADI O, HORVATH O, MARCSIK A, MOLNÁR E, PALFI GY.
Healing and Sexual Symbolism - Avar Trephinations in the 7-9th Century AD Carpathian Basin.

In: McGlynn, George; Kirchengast, Sylvia; Zink, Albert; Grosskopf, Birgit (szerk.) 11th Meeting of the Society for Anthropology (GfA). Evolutionary and Modern Challenges to Homo sapiens – An Anthropological Inquiry. Abstract and Program Booklet
München, Németország (2015) 105 p. pp. 15-15, 1 p.

VARADI O, TIHANYI B, HORVATH O, MARCSIK A, MOLNAR E, PALFI GY, BERECZKI ZS.
Symbolic trephinations of extraordinary shape in the Carpathian Basin.
In: Gál, Szilárd Sándor (szerk.) 1st Conference of the Anthropological Association "Aurél Török"
Târgu-Mureş, România (2015) pp. 6-6, 1 p.

VARADI O, HORVATH O, BERECZKI ZS.
Szilvamag alakú jelképes trepanációk a Kárpát-medencében.
In: Mesterházy, B (szerk.) XIII. Természet-, Műszaki és Gazdaságtudományok Alkalmazása Nemzetközi Konferencia: Előadások: 13th International Conference on Applications of Natural, Technological and Economic Sciences: Proceedings from Conference
Szombathely, Magyarország: Nyugat-magyarországi Egyetem, Természettudományi és Műszaki Kar, Természetföldrajzi Tanszék, (2014) pp. 25-25, 1 p.